Image Reduction Pipeline for the Detection of Variable Sources in Highly Crowded Fields

Claus A. Gössl, Arno Riffeser

Universitäts-Sternwarte München, Scheinerstraße 1, D-81671 München

Abstract. We present a reduction pipeline for CCD (charge-coupled device) images which was built to search for variable sources in highly crowded fields like the M 31 bulge. We describe all steps of the standard reduction including per pixel error propagation: Bias correction, treatment of bad pixels, flatfielding, and filtering of cosmic ray events. We utilize a flux and PSF (point spread function) conserving alignment procedure and a signal-to-noise maximizing stacking method. We build difference images via image convolution with a technique called OIS (optimal image subtraction, Alard & Lupton 1998), proceed with PSF-fitting, relative photometry on all pixels and finally apply an automatic detection of variable sources. The complete per pixel error propagation allows us to give accurate errors for each measurement.

1. Introduction

The WeCAPP project (Riffeser et al. 2001) which aimed at the M 31 bulge to search for Microlensing events yielded 0.2 TB of inhomogenous raw imaging data. Available data reduction software was not able to comply with the highly variable observing conditions (varying seeing, skylight background, and flatfield quality; different cameras, CCDs, and telescopes) and yet give consistent measurements with reliable error estimates. Therefore we decided to develope our own reduction pipeline. (For additional information on and motivation of error propagation see also Moshir et al. [O9.2] and Gössl & Riffeser 2002.)

2. The Reduction Pipeline

2.1. Bad Pixels & Bias Correction

We mask saturated (and blooming affected) pixels, as well as CCD-defects (hot, cold pixels etc.). We subtract the bias level of individual frames estimated from the overscan region and a masterbias ($\kappa\sigma$-clipped mean image of multiple bias level corrected bias frames).

2.2. Initial Error Estimate

The initial error estimate for each pixel in every image is calculated from the pixel's photon noise ($\sqrt{\mathrm{signal/gain}}$), the bias noise of the image (clipped RMS of the overscan), and the uncertainties of bias level and bias pattern determination.

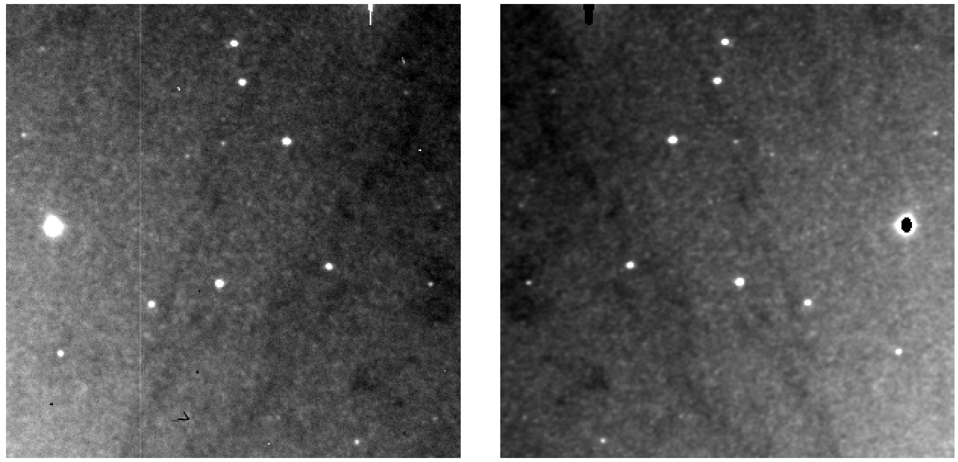

Figure 1. Left: This (300 × 300 pixels) window of a raw CCD image from a part of the M 31 bulge was taken at the Calar Alto 1.23 m telescope, 3. Feb. 2001. (WeCAPP project, Riffeser et al. 2001.) Right: Stacked image after steps Sect. 2.1. to Sect. 2.5..

Errors are propagated throughout the complete reduction pipeline with Gaussian error propagation.

2.3. Flatfield Calibration

To achieve a high signal-to-noise ratio (S/N) for a combined flatfield of an epoch we first calculate in each pixel the error weighted mean of normalized and illumination corrected twilight flatfields. After rejecting all 5×5 pixels regions where the center pixel exceeds this mean by more than 5σ, the final calibration image is built by 3σ clipping of the remaining pixels.

2.4. Cosmic Ray Rejection

We fit five-parameter Gaussians to all local maxima of an image. Sources with a width along one axis of the fitting function smaller than a threshold (which has to be chosen according to the PSF) and, in addition, an amplitude of the fitting function exceeding the expected noise by a certain factor (which has to be chosen according to the additional noise i.e. due to crowding) correspond to cosmics. We mask the pixels, where the fitting function exceeds the fitted surface constant by more than two times the expected photon noise.

2.5. Image Alignment & Stacking

Images are shifted onto a reference grid using a flux and PSF conserving algorithm. The shifted images are photometrically calibrated using the profile of the M 31 bulge. Bad pixels (except saturated) are replaced with pixels of the most similar image, but accounted for in the error image. The final stack is built by maximizing its S/N ratio using the error images and the PSF width for the calculation of weighting factors (Fig. 1).

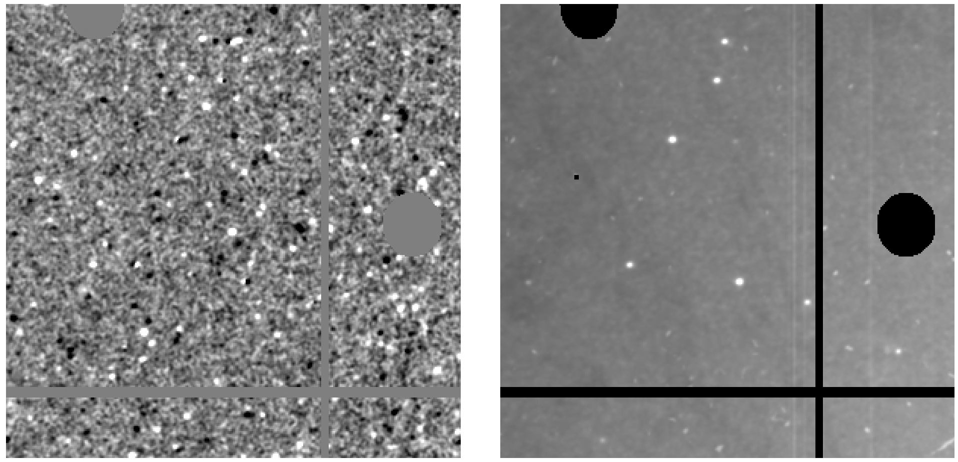

Figure 2. Left: Profile fitting photometry (cuts: $-5 \cdot 10^{-6}$ Jy, $+5 \cdot 10^{-6}$ Jy). Right: Corresponding error frame (cuts: $+0.6 \cdot 10^{-6}$ Jy, $+1.2 \cdot 10^{-6}$ Jy).

2.6. Image Convolution & Reference Subtraction

For the difference photometry a high S/N reference frame with a narrow PSF is convolved to the broader PSF of each science frame. The calculation of the convolution kernel is performed by a least squares linear fitting procedure optimizing 52 free parameters (OIS). The difference frame (build by subtracting the convolved reference frame from the science frame) shows a large amount of positive and negative point sources.

2.7. Variable Sources Detection

Fluxes for the variable sources are extracted using PSF-fitting photometry in each pixel: The PSF of a high S/N star in the convolved reference frame is fit to a small region around each pixel in the difference image (Fig. 2). This reduces the influence of neighboring variable sources to a low level. Therefore we are able to extract light curves for each pixel of the difference frame (Fig. 3).

3. The Implementation

All algorithms are implemented in C++. Each individual reduction step is represented by a commandline program. The pipeline is a simple shell script or Makefile. We take part in the developement of a Little Template Library (LTL) which provides very fast and easy to use methods for I/O (i.e. FITS or ASCII), array operations, statistics and Linear Algebra as well as for commandline flags and configuration file parameters.

Acknowledgments. Our thanks are due to Ralf Bender, Niv Drory, Jürgen Fliri, Ulrich Hopp, and Jan Snigula. This work was supported by the German *Deutsche Forschungsgemeinschaft, DFG*, SFB 375 Astroteilchenphysik.

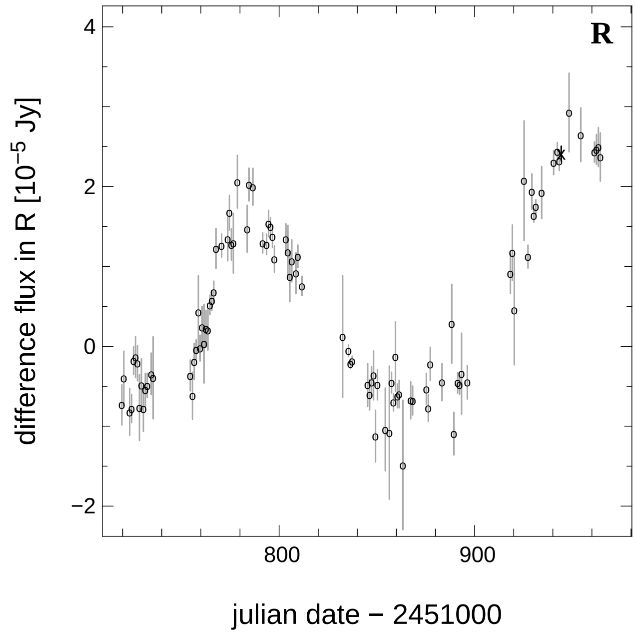

Figure 3. Final light curve of a long periodic, semi-regular variable star (in the center of Fig. 2). The '×' displays the epoch of the sample images. The sample source in the sample image shows a difference flux of $2.4(\pm 0.1) \cdot 10^{-5}$ Jy on a background of $11 \cdot 10^{-5}$ Jy / arcsec^2.

References

Alard, C., & Lupton, R. H. 1998, ApJ, 503, 325

Gössl, C. A., & Riffeser A. 2002, A&A, 381, 1095

Moshir, M., Fowler, J., Henderson, D. this volume [O9.2]

Riffeser, A., Fliri, J., Gössl, C. A., Bender, R., Hopp, U., Bärnbantner, O., Ries, C., Barwig, H., Seitz, S., Mitsch, W. 2001, A&A, 379, 362